TOWARDS AUTOMATIC DTM VERIFICATION EXPLOITING STEREO ORTHOPHOTOS

Michael Hahn
Institute for Photogrammetry – Stuttgart University
Keplerstraße 11, D-7000 Stuttgart 1
Commission III

Abstract

Automatic procedures exist for the acquisition of Digital Terrain Models (DTMs) from digital images as well as for the computation of digital orthophotos. Both, DTM and orthophoto, are frequently derived within a common framework, in which the human operator plays a minor role. The situation is just inverse with regard to the verification process. The usual way is to superimpose a wireframe or contour line representation of the DTM onto the stereo images. Then the verification is carried out step by step by detailed visual control.
Quality control and verification of digital terrain models have always been a problem. It is getting more demanding with regard to the automatic generation of DTMs by digital image matching, as also the verification should be automatic as far as possible.
In this paper we outline possibilities of automatic DTM verification using stereo orthophotos. The automatic verification is approached by exploiting the intensity differences between the stereo partners. Three different ways are discussed based on (1) regression analysis, (2) modelling radiometric differences by finite elements and (3) generation of orthophoto pyramids. All three approaches result in a segmentation of the DTM into usually small areas, which are not represented completely by the model and the large remaining area which is consistent with the imaged world. Experimental results of simulations and real data indicate that by the computationally more efficient approaches (1) and (3) the misrepresented areas are located with higher significance than with the finite element procedure (2).

Keywords: Image Analysis, DTM, Orthophoto, Stereoscopic, Data Quality, Verification, Image Interpretation

1 INTRODUCTION

Digital terrain models and orthophotos

Today digitization and digital processing of images are considered to be the basis for developing procedures which automatically produce standard products of photogrammetry. The term "automation" seems to be inherently attached to the technical development of each time period, even though the quality of automation increases usually and often previously reached progress is incorporated in the actual one. In the last decade remarkable progress is achieved especially in the acquisition of digital terrain models (DTMs). Numerous presented papers discuss procedures, in which the manual measurement process is taken over from techniques of image matching. In connection with the algorithms for surface interpolation this leads to procedures in which the human operator plays a minor rule. The reconstruction processes presented recently, which solve the matching and interpolation step within one framework, work on the iconic level as well as the symbolic level of image description. State of the art is that many of these methods are checked by developing prototypes. Moreover some of the prototypes are implemented operationally and matured to productive systems (Ackermann and Krzystek, 1991).

A second standard product in photogrammetry are the orthophotos. In general there is a simple process of differential rectification in which the (aerial) photo is reprojected to be geometrically congruend to a map. In the case of digital imagery this geometric definition of a digital orthophoto still holds. Using the terrain model and the orientation of the image, the location of each picture element of the orthophoto can easily be transformed to the aerial image. The intensity value at this image point then can be found by resampling. In some applications the area represented by an orthophoto pixel is significantly larger than the area of an object represented by an image pixel, so that in this case strong smoothing accompanies resampling. This means, that the whole process is just a simple image processing procedure of differential resampling. If the area for which an orthophoto has to be produced is not covered by one aerial image, pieces have to be put together from the adjacent photos. Within this process, called mosaiking, adjacent images are adjusted radiometrically, for example, in order to smooth away linear steps (Jansa and Guangping, 1990). That such an adjustment is necessary results from a simple fact: the intensity values in orthophotos of the same scene, resampled from different images (taken from different positions in the world) are usually different. Assuming all geometric aspects (perspective projection, orientation, surface model) to be perfectly known, these differences reflect noise (which we consider to be a minor problem) and physical aspects of image formation. Unfortunately, the physical aspects of image formation we are concerned with correspond to the difficult question: what determines the intensity value at a particular point in the image and consequently in the orthophoto ? There is a whole chain of dependencies, which begins with the A/D converter characteristics of the scanner or the digital camera. Clearly how much energy arrives at a particular point in the image depends on the energy emitted from the surface, on the degree of absorption, on how the object is illuminated and how it reflects light. In most cases is assumed, that the reflectance model is a combination of a Lambertian model and a specular model.

In computer vision research some work is done to separate specular reflection components from Lambertian components (e. g. Coleman and Jain (1982) and Klinker, Shafer and Kanade (1988)). A few attempts have been made to directly extract parameters of either one or both of the reflectance models (e. g. Nayar, Ikeuchi and Kanade (1988) and Ikeuchi and Sato (1990). The experiments provided in these investigations are usually based on simulations.

Stereo orthophotos

The terms stereo orthophotos or stereo orthoimages we want to use in a distinct analogy to the term stereo images. From the two images taken in standard stereo configuration the two corresponding orthophotos are derived by the same procedure. The overlapping area in the images yields redundant orthophoto information pixel by pixel. These overlapping areas of both orthophotos are what we call the *stereo orthophotos*. To avoid confusion it is notable to say, that this is not in agreement with the understanding of the term stereo orthophotos as it is used in some textbooks of photogrammetry[1]. Originally the idea behind stereo orthophotos was to simplify the mapping process. For this a second copy of an orthophoto was generated, in which the image points are shifted with parallaxes reflecting the elevation model.

For updating existing maps Peterle (1989) uses orthophotos, which are derived from images taken of the same object but with a time lag of several years. This implies, that the scene in meantime in general has changed. Even though the mapping is of prior interest in this work, there are similarities to the verification task as we will see later.

Viewing the stereo orthophotos stereoscopically, as proposed by Finsterwalder (1985) mainly for orthophoto verification, can be an efficient way to verify the DTM manually. Just in the case of working at digital photogrammetric workstations this seems to be more promising than other techniques like superimposition of wireframe or contour line representations of the DTM on original stereo imagery. Up to now superimposition is realized only as an analog technique, applied in the environment of analytical plotters, which work with the photographs directly.

Verification

Without doubt the human endowment with the ability to see, to discern and locate objects, to reconstruct and understand the 3D space is the splendid pre-condition to do the verification of DTMs using stereo orthophotos. The geometric model for parallaxes between the orthophotos is just the expectation that the parallaxe at any point is zero. This is equivalent with the expectation, that the spatial impression gained from the stereo orthophotos is a planar object which corresponds to the plane of the orthoprojection. All spatial deviations from planarity, i. e. all nonzero parallaxes, indicate inconsistencies between the DTM and the real world surface.

With this paper we want to pick up the complex of automatic DTM verification. The way to develop a fully automatic DTM verification procedure is presumably quite long, because at least some of the human abilities of understanding images have to be incorporated in the procedure. A strategy to approach the verification task could be as follows:

(1) Detect intensity differences between the orthophotos. Supposed the orthophotos are generated in such a way that intensity values are obtained at identical location, the correspondence between the orthophoto pixels is implicitly given. In a simplest subtraction method, the intensities of each pixel of the stereo orthophotos are subtracted from each other. Significant nonzero values in the difference orthoimage indicate inconsistencies between the orthophotos. By aggregation of the affected pixels into areas, directly the location of doubtful areas is indicated. If we assume that the physical aspects of image formation addressed above are not the reason for these changes, then the differences can be interpreted as indication for discrepancies between real world geometry and DTM. More sophisticated methods than the simple subtraction are discussed in the next section.

(2) The areas of interest located in the first step may be hints for objects like trees, houses, or bridges which are not represented in the DTM. Furthermore structural information like breaklines or other discontinuities, which are not included in the measured data or which are smoothed out within surface interpolation, also might be the reason for the differences. Such errors and all other geometric errors which have not been recognized within the data capture or the interpolation process are candidates for areas of discrepancies. The interpretation involves modelling, reconstruction and location estimation of the 3D structure or shape of the objects or imperfections of the DTM. The next step is to decide if and if necessary which of the reconstructed information has to be included or eliminated from the existing DTM. In this classification constraining rules (e. g. do not represent mobile objects, trees, etc.) have to be incorporated. It is obvious that other informations like colour would be helpful if not even necessary to come to an automation of this interpretation task.

In this paper we present some work on the localization of conflicting regions between two orthophotos. The term localization as used in this context comprises the detection of discrepancies and, in consequence, the location of regions in the DTM which do not agree with the real world surfaces. The idea is to analyse the whole area covered by stereo orthophotos and locate the discrepant regions. These areas are marked and visualized, so that instead of a detailed visual control of the whole area we only have to carry out interpretation for a certain percentage point (e. g. 5 % or 1 %) of the total area. In the next section we briefly describe three different procedures for localizing discrepancies in the orthophotos and in the third section we will present results with simulated and real stereo imagery.

2 LOCALIZATION OF DISCREPANT REGIONS BETWEEN STEREO ORTHOPHOTOS

All procedures we describe work on the iconic level of image description, i. e. the intensities of the orthophotos are used for comparison. In consequence, the problem we have

[1]Sometimes the term stereo orthophotos is used to characterize two orthophotos which are derived from one image by orthoprojection along different spatial directions of projection, or which has the same effect, by shifting all image points of an orthophoto by parallaxes proportional to the elevation difference of the point over a reference plane (Blachut, 1971, Collins, 1968).

to solve is first to find a suited radiometric transformation between the orthoimages to eliminate systematic differences in the intensities which result from physical aspects of image formation. Secondly, if the systematic effects are eliminated, the resulting differences in the intensities can be tested. Those pixels where significant differences are indicated can be grouped together (applying region growing and closing to fill small gaps), so that the location of this discrepant regions in the orthoimages and with them in the DTM is found. Assumed to be given two digital (aerial) intensity images together with the complete interior and exterior orientation, and a digital terrain model. The first we do is to compute orthophotos from each of the two images individually thereby taking the same regular lattice. In consequence the geometrical prerequisites for comparing pixels are fulfilled. The differential resampling is done for each orthophoto pixel individually by computing the corresponding position in the aerial image and resampling with the sinc-function. That this involves great expense is quite clear. But for the experimental investigations we want to avoid approximations in this first step.

The procedures which we explore for localization of discrepancies consist of radiometric transformation models between the stereo orthoimages and thresholding. The intensities of the orthoimages 1 and 2 are denoted by $O_1(r,c)$ and $O_2(r,c)$, respectively. For model A we assume linear regression with radiometric scale and shift parameter according to

$$\text{A:} \qquad O_1(r,c) + \epsilon(r,c) = \hat{a} O_2(r,c) + \hat{b} \,.$$

The adjustment with two parameters allows to compensate only global differences between the intensities if the images. This model does not differ from a direct subtraction procedure significantly.

For model B we assume that the intensity differences between the stereo orthophotos can be described by a finite element (FE) model, which we formulate by

$$\text{B:} \qquad \begin{aligned} O_1(r,c) + \epsilon_1(r,c) &= \hat{O}(r,c) \\ O_2(r,c) + \epsilon_2(r,c) &= \hat{O}(r,c) + \alpha(r,c,m,n)\, \hat{C}(m,n) \,. \end{aligned}$$

The adjusted "parameters" $\hat{O}(r,c)$ differ from orthoimage O_1 by the estimated residuals, which reflect noise if model B is true. The grid spacing of the adjusted difference surface $\hat{C}(m,n)$ between O_1 and O_2 is a multiple of the grid spacing of the orthophoto lattice. The finite elements of C are facets with bilinear surfaces, i. e., all orthoimage pixels (r,c) contribute according to their weights in the bilinear interpolation operator $\alpha(r,c,m,n)$ to the determination of $\hat{C}$. The individual facets are connected to the neighbouring facets by joint edges and identical node values $\hat{C}(i,k)$. In comparison with model A the FE-model is more flexible because the surface C is able to follow the differences between O_1 and O_2 up to a certain degree. The formulation of radiometric surface models has e. g. also been proposed by Wrobel (1988) in the context of DTM reconstruction and orthophoto generation from digital imagery.

For the third procedure no explicit model for parameter estimation has to be formulated. The idea behind is quite different from A and B. We propose working with image pyramids applied to the orthophotos. In consequence the construction of orthophoto pyramids is the first step. For that purpose the images are smoothed with a Gaussian filter with radius 1 and resampled to obtain the next level of the pyramid. The resampling operation reduces the number of pixels by the factor 2×2 to 1 which fits to the Gaussian diameter of 2 pixels. In this way the pyramid is generated. We count the levels from the bottom to the top, i. e. level 0 of the pyramid bears the original image and level n is the coarsest representation level for the image information. To get an idea on a variety of applications which use image pyramids refer e. g. to Ackermann and Hahn (1991) and Rosenfeld (1984).

From each of the stereo orthophotos an image pyramid can be constructed. Computing the differences between the pyramids for all levels gives a difference orthophoto pyramid (DOP). On the coarser levels of this DOP low frequent information is represented which matches with global differences between the orthophotos. Because inconsistencies between the DTM and the real world geometry are of local nature (if not, then this DTM appears not to be a suited model to represent the surfaces of the corresponding world), this local differences will be mixed with the global ones. So it suggests itself to eliminate the coarse level differences from the information of the next refinement level. This procedure we formulate by

$$\begin{aligned} \text{C:} \qquad & \text{calculate } DOP_i \text{ for all levels } i \\ \text{eliminate } DOP_k & \text{ from the current level } k-1: \\ & DOP'_{k-1} = DOP_{k-1} - DOP_k \end{aligned}$$

By this technique we get a bandpass copy of the intensity differences between the stereo orthophotos. Depending on the spatial extend, the discrepancies are expected to be indicated mainly on the first few levels of the bandpass copy.

For all three models A,B,C the stochastic component, i. e. the noise in the orthoimage intensities, is assumed to be white Gaussian noise.

In the models A and B the error terms ϵ and the difference surface $\hat{C}$, in model C the elements of the bandpass DOP are tested and thesholded. As described before it will be more convenient to visualize the discrepant regions rather than individual pixels. Therefore region growing should be applied as a final step.

3 EXPERIMENTS AND RESULTS

For the experimental investigations we pick up an image pair, which was used by Hahn and Förstner (1988) to assess the quality of matching procedures applied for DTM reconstruction. Though the radiometric differences in the intensities are considerable, as is convincingly shown in figure 1, with the matching algorithms a DTM precision of better than 0.2 % of the flying height h was obtained in this project. For two other projects with less demanding surface geometry the precision was around 0.1 % of h. For presentation of the results we chose two characteristic examples for each of the three procedures A,B,C described above. More examples are collected in Raißer (1991).

For the first test we simulate the imaging process. The DTM, the orientation of two images and an orthophoto are given and the two images are generated by resampling from the orthophoto. For each of the image pixels the corresponding point location in the orthophoto is found iteratively by a numerical difference scheme. Consequently the only differences between this two images are of geometric nature. Now an error is introduced into the DTM and the stereo orthophotos are derived using the imagery found by the simulated imaging process. The differences between the stereo orthophotos are directly (uniquely) the consequence of the error in the DTM. The results applying the linear regression model (A), the FE-procedure (B) and the DOP-procedure (C) are shown in figures 2, 3 and 4, respectively.

That the error is very well indicated by procedure A (figure 2) could be expected, because the idealized assumptions of the simulated imaging process fit well to the simple model. Because of this the form of the introduced DTM error which approximates a cross can be seen quite nice in figure 2. In exactly five neighboring points of the DTM an error of 3 m in elevation is added. More surprising is that with the FE-procedure just in this case difficulties arise. The residual images ϵ_1 and ϵ_2 show noise as expected. In the difference surface (figure 3), for which in the case of this figure a grid spacing of 5 times the orthophoto pixel size is chosen, the error can be recognized but much less distinct than expected. Coarsening the resolution of this difference surface amplifies the visual impression of the error but up to a spacing distance of 10 times the pixel size. For larger spacing distances the response in the difference image is lost. Neglecting the fine grained lowest level of the DOP, the next three bandpass levels of the DOP (figure 4) all indicate the error. So with procedure A and C the approximate position of the error is simply located and roughly size and form of the erroneous region could be found.

The second test then uses the two images without modification, i. e. just as they have been digitized from the aerial photos (figure 1). From these two images the corresponding orthophotos are derived by differential resampling. The same DTM with the identical error as in the first test with the simulated idealized imaging process was used. The stereo orthophotos are plotted in figure 5. If viewing this image pair stereoscopically the DTM error as well some trees which are not represented in the DTM can be observed. The results applying the linear regression model, the FE-procedure and the DOP-procedure again are shown in figures 6, 7/8 and 9, respectively.

The residual image which results from linear regression gives some indications about the DTM errors as can be seen from figure 6. Plotted in this figure is the thresholded residual image, i. e. only those residuals which are larger than two times the standard deviation. The black blobs in the lower left and right of this image correspond to trees. Figure 7 gives an impression of a residual image estimated by the FE-approach. Typical for this FE-residuals is that, as can be seen in figure 7, only noise is present. The difference surface (figure 8) shows large systematic differences between the two orthophotos. Hardly to recognize are some indications to trees, and practically nothing is to see from the DTM error in this data. The last images (figure 9) show the first four bandpass levels of the DOP. On the coarse levels 2 and 3 the trees can be recognized. The DTM error shows up slightly on level 2.

in total, this real example reveals considerable problems which arise when the radiometric distortions between the images are large. If the radiometric transformation is very flexible as in the case of the FE-model, the resulting error terms indicate that the transformation works satisfactory. Unfortunately the situation for localizing DTM errors in this case is just inverse, i. e. the errors are also taken away with the transformation. More promising are the more simple procedures based on regression as well as on image pyramids.

4 CONCLUSION

In this paper we followed a pragmatic line of investigation: at first we have explored some experiments to gain insight into problems we meet on the way to automatic DTM verification. To eliminate differences between stereo orthophotos arising from distinct physical processes we used a simple model based on linear regression and a more complex procedure based on modelling differences by a finite element surface. The idea behind the third procedure is multiscale (bandpass) analysis, used to separate events arising at different scales.

The example chosen for this experiments are real images with considerable radiometric differences. In summary, with this image data, all three procedures have problems in detecting inconsistencies, which result from differences between real world geometry and the DTM. The more complex FE-approach seems to eliminate too much, so that nearly no hints to the DTM errors remain. The more simple and computational more efficient approaches based on regression analysis as well as on bandpass DOPs seem to be more promising. This especially holds true for imagery in which systematic differences between the image intensities are small. The results found based on the simulated imaging process support this observation.

One direction of future work is to explore the information inherent in the symbolic level of image representation. Though our first experiments with edge images have not been very encouraging, we expect that the less sensitivity to physical effects will lead to an improvement for the verification task.

REFERENCES

Ackermann, F., Hahn, M. (1991): Image Pyramids for Digital Photogrammetry. In: Ebner, H. et al.: Digital Photogrammetric Systems, Wichmann-Verlag, Karlsruhe.

Ackermann, F., Krzystek, P. (1991): MATCH-T: Automatic Mensuration of Digital Elevation Models. Presented paper to the 3rd Technical Seminar of Sociedad Espanola de Cartografia, Fotogrametria y teledeccion, Barcelona.

Blachut, T.J. (1971): Stereo-Orthophoto Systems. Bildmessung und Luftbildwesen 39, S. 25-28

Coleman, E.N., Jain, R. (1982): Obtaining 3-dimensional Shape of Textured and Specular Surface using four-source Photometry. Computer Graphics and Image Processing, 18(4).

Collins, S.H. (1968): Stereoscopic Orthophoto Maps. Canadian Surveyor 22, pp. 167-176.

Finsterwalder, R. (1985): Orthophoto-Selbstkontrolle. Bildmessung und Luftbildwesen 53 (3), S. 72-74.

Hahn, M., Förstner, W. (1988): The Applicability of a Feature Based and a Least Squares Matching Algorithm for DEM-Acquisition. IAPRS 27(B9), Kyoto.

Ikeuchi, K., Sato, K. (1990): Determining Reflectance Parameters using Range and Brightness Images. 3. Intl. Conf. on Computer Vision, Osaka.

Jansa, J., Guangping, H. (1990): Eine radiometrische Anpassungsmethode für die Mosaikherstellung aus digitalen Bildern. Zeitschrift für Photogrammetrie und Fernerkundung, 58(2).

Klinker, G.J., Shafer, S.A., Kanade, T. (1988): The Measurement of Highlights in Color Image. International Journal of Computer Vision, 2(1).

Nayar, S.K., Ikeuchi, K., Kanade,T. (1988): Extracting Shape and Reflectance of Lambertian, Specular and Hybrid Surfaces. Tech. Rep. CMU-RI-TR-88-14, Carnegie Mellon University.

Peterle, J. (1989): Fortführung topographischer Karten mit Methoden der digitalen Bildverarbeitung. Diss. Univ. Karlsruhe, 1989.

Raißer, M. (1991): Überprüfung digitaler Höhenmodelle anhand von Orthophotos. Master thesis at Stuttart University, unpublished.

Rosenfeld, A. (Ed) (1984): Multiresolution Image Processing and Analysis. Springer Series in Information Sciences, Vol. 12.

Wrobel, B.P. (1988): Least Squares Methods for Surface Rekonstruction from Images. Proc. of ISPRS, Comm. III, Kyoto, Japan.

Figure 1: Stereo image pair with histograms

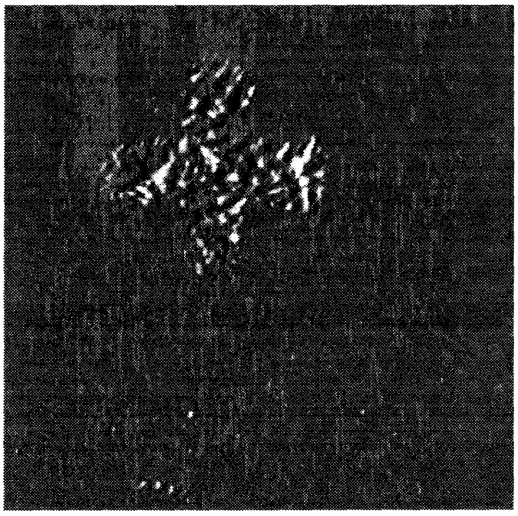

Figure 2: Residual image resulting from the linear regression procedure A

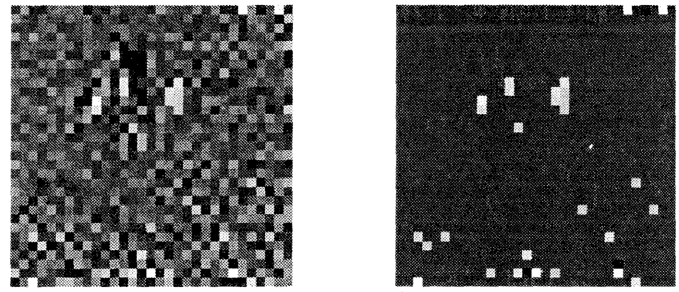

Figure 3: Radiometric difference surface estimated by the FE-approach B. On the right the thresholded differences are plotted additionally.

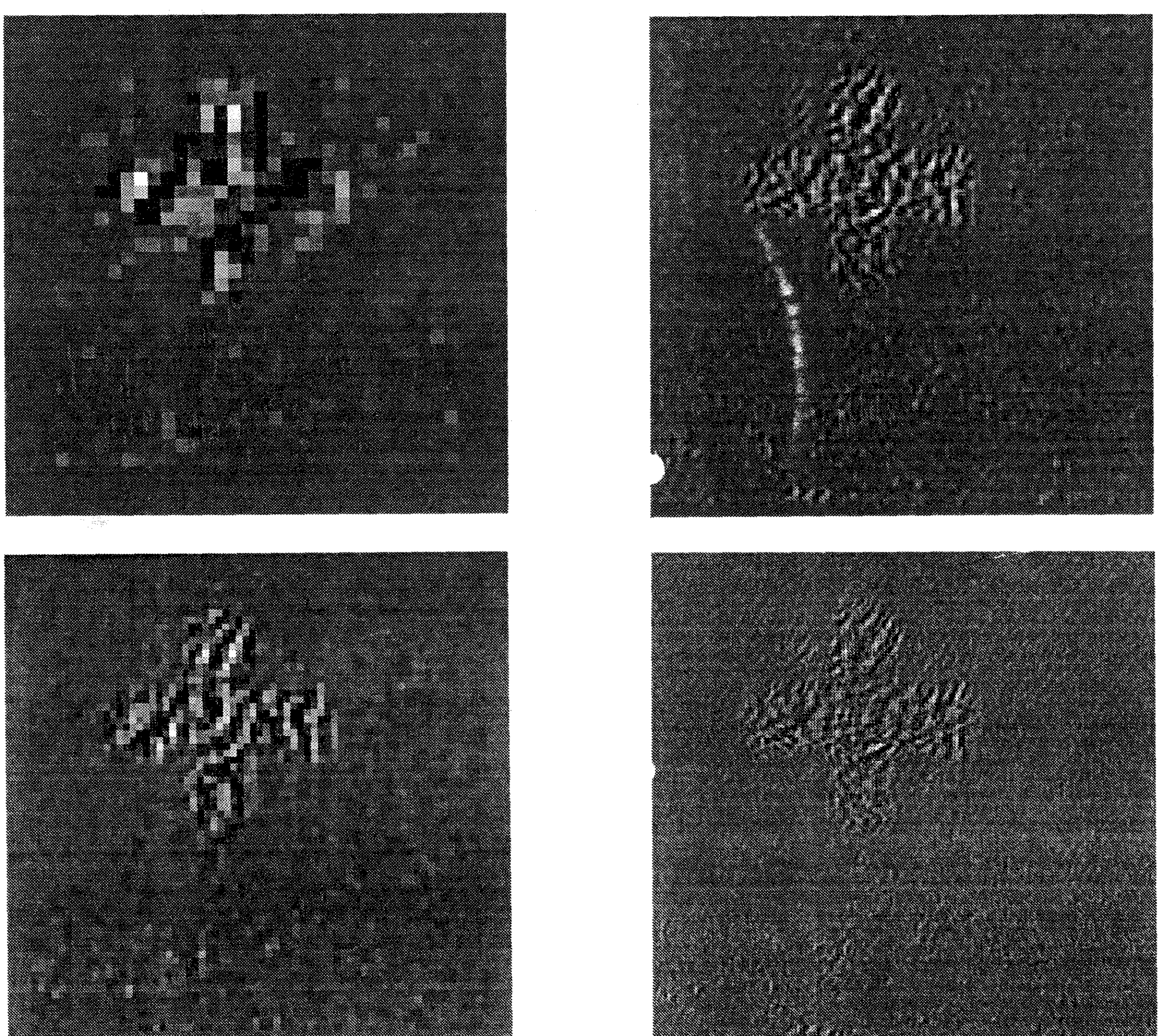

Figure 4: The levels 0 to 3 of DOP'_k of the DOP-procedure C

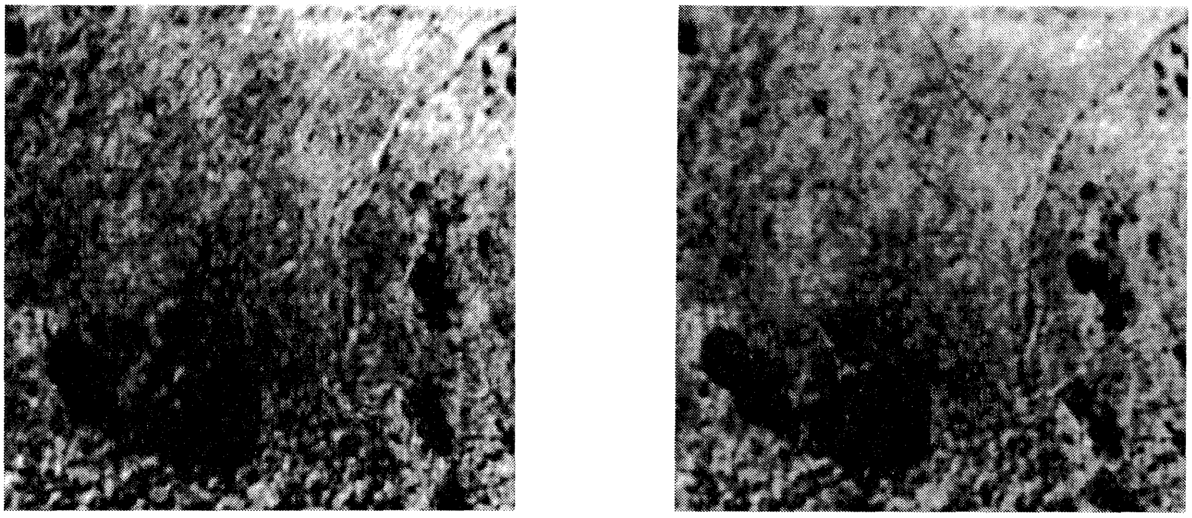

Figure 5: Stereo orthophoto images: with stereoscopic viewing the DTM error as well as some trees can be recognized.

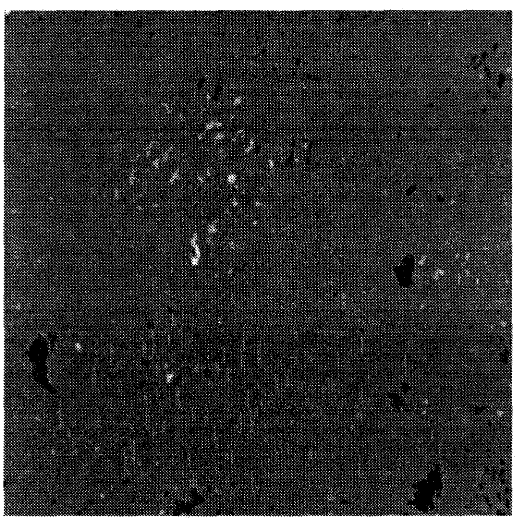

Figure 6: Residual image found by linear regression

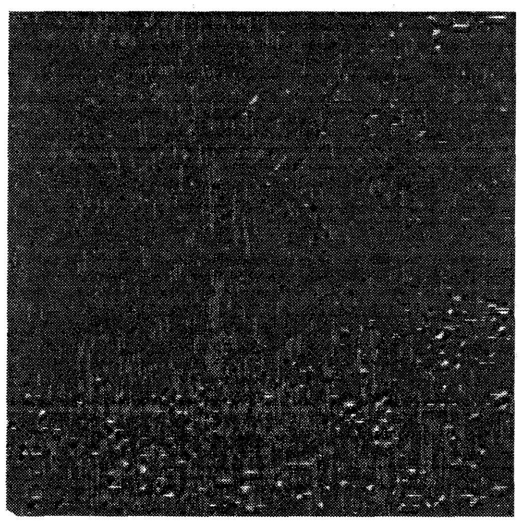

Figure 7: Residual image resulting from the FE-approach

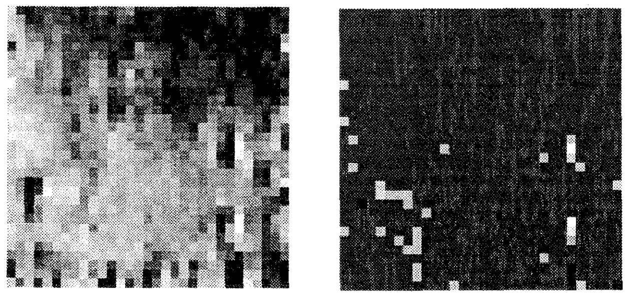

Figure 8: Difference surface estimated by the FE-approach.

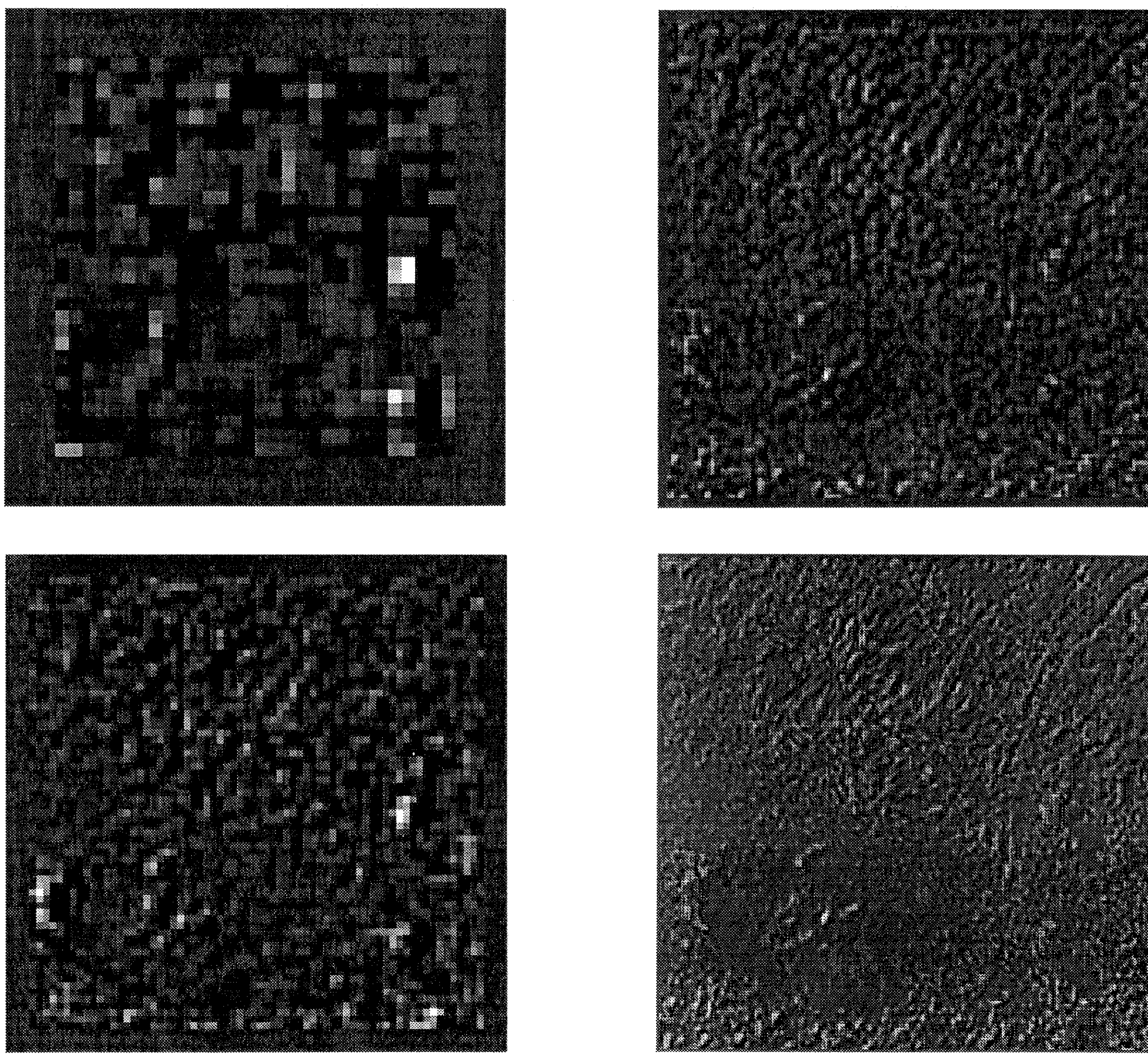

Figure 9: The DOP_k' levels 0 - 3 of the DOP-procedure